2009 American Control Conference
Hyatt Regency Riverfront, St. Louis, MO, USA
June 10-12, 2009

Estimation of Road Friction for Enhanced Active Safety Systems: Dynamic Approach

Changsun Ahn, Huei Peng, and H. Eric Tseng, *Member, IEEE*

***Abstract*—Frictional coefficient between tire and road is difficult to detect but crucial for vehicle active safety systems. Several approaches for friction coefficient estimation were developed based on various vehicle dynamic phenomena. This paper suggests nonlinear state observers that use vehicle dynamics, steering system dynamics, and tire force dynamics as a viable approach. The stability of the observer highly relies on observer gains. We present two different ways to select the gains and discuss the stability of the observer. Furthermore, we introduce a hybrid estimator which uses a nonlinear observer and a nonlinear least square method which provides enhanced performances. These estimators are verified using the commercial software, Carsim, under various scenarios.**

I. Introduction

TIRE forces and road friction coefficient are important information for vehicle safety warning and control systems because tire forces are limited by the frictional coefficient. Road friction can change by an order of magnitude between normal and icy conditions, which means the vehicle response will change dramatically and the control/observer gains need to change significantly. Many algorithms for friction estimation have been developed [1]-[7]. Ahn [1] and Hsu [2] used nonlinear least square methods to detect frictional coefficient. Nonlinear least square method requires more computational load than a dynamic based observer. As mentioned in [1], vehicle lateral motion is more robust to disturbances than wheel motion, and the information about lateral motion is available if the vehicle has ESP (Electronic Stability Program). Furthermore, the increasing adaptation of electric power assisted steering system makes it possible to measure self-aligning torque of the front tires. Recently, Toyota published a series of papers [8]-[11] presenting measurement and estimation of self-aligning torque, with encouraging experimental results. These papers showed the possibility of vehicle/road parameter estimation using front tire aligning torque.

Robustness and cost consideration lead us to focus on a nonlinear observer using vehicle lateral dynamics and front tire dynamics as the basis of estimation. Nonlinear observers are used to accommodate nonlinear tire model with simple tuning parameters, i.e., observer gains. There is a lot of previous research on nonlinear observers. Canudas-de-wit [3] used lumped longitudinal dynamics with LuGre model which is only based on wheel speed signal. Hsu [4] suggested a nonlinear observer using an adaptive gain, but no stability proof was given. Ray [5] estimated tire forces and friction using extended Kalman-Bucy Filter without an explicit friction model. Baffet [6] estimated side slip angle and tire forces with extended Kalman filter based on a four-wheel vehicle model and adaptive linear tire force model. Dakhlallah [7] used extended Kalman Filter based on four wheel vehicle model and Dugoff tire model to estimate tire forces and sideslip angle. However, these extended Kalman Filter based observers also do not show stability proof.

In this paper, firstly, we introduce a nonlinear observer based on linear vehicle model and nonlinear tire force/torque model with lateral acceleration and self-aligning torque measurement, the stability conditions for the observer is then derived. The stability conditions serve as guideline for the selection of observer gains. With the guideline we suggest two different methods for gain selection, adaptive gain and robust gain. The advantages and limitations of the two methods are analyzed. Finally, we present a hybrid method to combine the nonlinear observer and nonlinear least square methods for improved performance. The stability and performance of the observers are verified with computer simulation under various road friction conditions.

II. System Models

Assuming pure lateral slip and constant longitudinal speed, a vehicle bicycle model effectively represents lateral and yaw dynamics of a two-axle ground vehicle with the following dynamics equations:

$$\begin{aligned} m(\dot{v}+ur) &= F_{yf}+F_{yr}, \\ I_z\dot{r} &= aF_{yf}-bF_{yr}, \end{aligned} \tag{1}$$

where u is the vehicle forward speed, v is the vehicle lateral speed, r is the yaw rate, m is the vehicle mass, I_z is the yaw moment of inertia. F_{yf} and F_{yr} are the lateral force at the front and rear axis, respectively. δ is the front wheel steering angle, and a and b are the distance from the vehicle center of gravity to front and rear axles. By using simple kinematics, we can

Manuscript received September 14, 2008. This work was supported by Ford Motor Company.

C. Ahn is with the Department of Mechanical Engineering, University of Michigan, Ann Arbor, MI 48109, USA (phone: 734-647-9732; e-mail: sunahn@umich.edu).

H. Peng is a professor of the Department of Mechanical Engineering, University of Michigan, Ann Arbor, MI 48109, USA (e-mail: hpeng@umich.edu).

H. E. Tseng is a technical leader of the Powertrain Controls Research & Advanced Engineering, Ford Motor Company, Dearborn, MI 48121 USA (e-mail: htseng@ford.com).

write α_f and α_r, slip angles of front and rear tires, in terms of u, v, and r:

$$\begin{aligned} \alpha_f &= (v + ar)/u - \delta, \\ \alpha_r &= (v - br)/u. \end{aligned} \tag{2}$$

Tire brush model is a simple tire model suitable for friction estimation purposes. Tire lateral force (f_y) and self-aligning torque (τ_a) are expressed as functions of tire slip angle, α, and frictional coefficient, μ below

$$f_y = \begin{cases} -3\mu F_z \gamma \left\{ 1 - |\gamma| + \frac{1}{3}(\gamma)^2 \right\}, & for\ |\alpha| \le \alpha_{sl} \\ -\mu F_z sgn(\alpha), & for\ |\alpha| > \alpha_{sl} \end{cases}, \tag{3}$$

$$\tau_a = \begin{cases} \mu F_z t \gamma \left(1 - 3|\gamma|\right)^3, & for\ |\alpha| \le \alpha_{sl} \\ 0, & for\ |\alpha| > \alpha_{sl} \end{cases}, \tag{4}$$

where $\gamma =: \theta_y \sigma_y$, $\alpha_{sl} =: \tan^{-1}(1/\theta_y)$, $\theta_y =: C_{\alpha f}/(3\mu F_z)$, $\sigma_y =: \tan(\alpha)$, t is the half of tire contact length, α is the tire slip angle, μ is the tire-road frictional coefficient, F_z is the tire normal force, and $C_{\alpha f}$ is the cornering stiffness of the tire.

III. Nonlinear Observer

The dynamics of front tire slip angle are derived from (1) and (2). Assuming constant road friction, the overall dynamics are

$$\dot{\alpha}_f = \left(\frac{1}{mu} + \frac{a^2}{I_z u} \right) F_{yf} + \left(\frac{1}{mu} - \frac{ab}{I_z u} \right) F_{yr} - r - \dot{\delta}, \tag{5}$$

$$\dot{\mu} = 0. \tag{6}$$

A nonlinear observer with linear error correction terms can then be derived:

$$\begin{aligned} \dot{\hat{\alpha}}_f = &\left(\frac{1}{mu} + \frac{a^2}{I_z u} \right) \hat{F}_{yf} + \left(\frac{1}{mu} - \frac{ab}{I_z u} \right) \hat{F}_{yr} - r - \dot{\delta} \\ &+ L_{11} \left(ma_y - \left(\hat{F}_{yf} + \hat{F}_{yr} \right) \right) + L_{12} \left(\tau_a - \hat{\tau}_a \right), \end{aligned} \tag{7}$$

$$\dot{\hat{\mu}} = L_{21} \left(ma_y - \left(\hat{F}_{yf} + \hat{F}_{yr} \right) \right) + L_{22} \left(\tau_a - \hat{\tau}_a \right), \tag{8}$$

where L_{11}, L_{12}, L_{21}, L_{22} are observer gains and elements of observer gain matrix L. The key problem for observer design is gain selection. We suggest two methods in the following.

A. Stability Conditions

To analyze the stability of the observer, we linearize (5), (6), (7), and (8). Let fn_1 be the right-hand side of (5), fn_2 be the right-hand side of (6), and $F \equiv F_{yf} + F_{yr}$ for convenience. Then, the linearized dynamics along a trajectory are

$$\begin{cases} \dot{x} = Ax + Bu \\ y = Cx \end{cases}, \tag{9}$$

where

$$x = \left[\alpha_f,\ \mu \right]^T,\ u = \left[r,\ \dot{\delta} \right]^T,\ y = \left[ma_y,\ \tau_a \right]^T,$$

$$A = \begin{bmatrix} \frac{\partial fn_1}{\partial \alpha_f} & \frac{\partial fn_1}{\partial \mu} \\ \frac{\partial fn_2}{\partial \alpha_f} & \frac{\partial fn_2}{\partial \mu} \end{bmatrix},\ B = \begin{bmatrix} -1 & -1 \\ 0 & 0 \end{bmatrix},\ C = \begin{bmatrix} \frac{\partial F}{\partial \alpha_f} & \frac{\partial F}{\partial \mu} \\ \frac{\partial \tau_a}{\partial \alpha_f} & \frac{\partial \tau_a}{\partial \mu} \end{bmatrix}.$$

Equation (3) and (4) are first differentiable at all x so that A and C are available along any trajectory. Furthermore the linear Luenberger observer for this plant is

$$\dot{\hat{x}} = A\hat{x} + Bu + L(y - \hat{y}) \tag{10}$$

$$\dot{\hat{x}} - \dot{x} = (A - LC)(\hat{x} - x) \tag{11}$$

Equation (11) indicates estimation error dynamics that is time varying because A and C matrices change as x varies along a trajectory. Stability of a linear time varying system is difficult to determine. However, if we assume, first, the state x stays in the linear region of (3) and (4), and second, A and B change slowly, then stability techniques of linear systems can be applied. Of course, the assumptions restricts the availability of these observer for some extreme maneuver cases. We will address the cases in future studies. If the real parts of all the eigen-values of A-LC are negative, then the stability of the observer is ensured. The eigen-values are solved from

$$\begin{aligned} \det(sI - A + LC) &= \det(sI - D) \\ &= s^2 - (D_{11} + D_{22})s + D_{11}D_{22} - D_{12}D_{21}, \end{aligned} \tag{12}$$

where

$$D = A - LC = \begin{bmatrix} D_{11} & D_{12} \\ D_{21} & D_{22} \end{bmatrix}.$$

The stability condition is

$$re\left(D_{11} + D_{22} \pm \sqrt{(D_{11} - D_{22})^2 + 4D_{12}D_{21}} \right) < 0, \tag{13}$$

i.e.,

$$\begin{aligned} &D_{11} + D_{22} \\ &\quad = A_{11} - L_{11}C_{11} - L_{12}C_{21} - L_{21}C_{12} - L_{22}C_{22} < 0, \end{aligned} \tag{14}$$

$$\begin{aligned} &D_{11}D_{22} - D_{12}D_{21} \\ &\quad = \left(A_{11} - L_{11}C_{11} - L_{12}C_{21} \right)\left(-L_{21}C_{12} - L_{22}C_{22} \right) \\ &\quad - \left(A_{12} - L_{11}C_{12} - L_{12}C_{22} \right)\left(-L_{21}C_{11} - L_{22}C_{21} \right) > 0. \end{aligned} \tag{15}$$

These two stability conditions serve as guidelines for selecting observer gains. Two methods are suggested below.

B. Adaptive Gains

The stability conditions easily can be achieved because we have four gains to satisfy two equations. For example, if we choose gains as follows:

$$L_{11} = C_{11} + \frac{A_{11}}{C_{11}}, \quad L_{12} = C_{21}, \quad L_{21} = C_{12}, \quad L_{22} = C_{22}, \tag{16}$$

then

$$D_{11} + D_{22} = -C_{11}^{\,2} - C_{21}^{\,2} - C_{12}^{\,2} - C_{22}^{\,2} < 0, \tag{17}$$

$$\begin{aligned} D_{11}D_{22} - D_{12}D_{21} &= \left(C_{11}C_{22} - C_{12}C_{21}\right)^2 \\ &+ \left(A_{12} - (C_{12}/C_{11})A_{11}\right)\left(C_{12}C_{11} + C_{22}C_{21}\right) > 0, \end{aligned} \tag{18}$$

because

$$\begin{aligned} &\left(A_{12} - (C_{12}/C_{11})A_{11}\right) \\ &= \left(\frac{1}{mu} + \frac{a^2}{I_z u}\right)\left(\frac{\partial F_{yf}}{\partial \mu} - \frac{\partial F/\partial \mu}{\partial F/\partial \alpha_f}\frac{\partial F_{yf}}{\partial \alpha_f}\right) \\ &+ \left(\frac{1}{mu} - \frac{ab}{I_z u}\right)\left(\frac{\partial F_{yr}}{\partial \mu} - \frac{\partial F/\partial \mu}{\partial F/\partial \alpha_f}\frac{\partial F_{yr}}{\partial \alpha_f}\right) = 0. \end{aligned}$$

The gains suggested in (16) result in

$$\begin{aligned} &L_{11} = \frac{\partial F}{\partial \alpha_f} + \frac{1}{mu} + \frac{a}{I_z u}\frac{\partial M}{\partial \alpha_f}\Big/\frac{\partial F}{\partial \alpha_f}, \quad L_{12} = \frac{\partial \tau_a}{\partial \alpha_f}, \\ &L_{21} = \frac{\partial F}{\partial \mu}, \quad L_{22} = \frac{\partial \tau_a}{\partial \mu}, \end{aligned} \tag{19}$$

where

$$F = F_{yf} + F_{yr}, \; M = aF_{yf} - bF_{yr}.$$

These gains are effective because they adapt to varying α_f, μ, and vehicle speed. However, there is a practical issue with this seemingly simple algorithm: these adaptive gains depend on the estimated α_f and estimated μ. In other words, there are additional dynamic interactions. The adaptive gains may not work satisfactorily if the current estimates are far from the actual values. When the road surface suddenly changes (e.g., hitting a patch of ice), the estimation might not be reliable, in a situation when we are in urgent need of accurate estimation.

C. Robust Gains

Another gain selection method is to choose a set of constant (robust) gains for robust stability of the observer, which may or may not be doable, depending on the range of uncertainties. To design the robust gains, we need to change the observer to (20) and (21).

$$\begin{aligned} \dot{\hat{\alpha}}_f &= \left(\frac{1}{mu} + \frac{a^2}{I_z u}\right)\hat{F}_{yf} + \left(\frac{1}{mu} - \frac{ab}{I_z u}\right)\hat{F}_{yr} - r - \dot{\delta} \\ &+ L_{11}\left(ma_y - \left(\hat{F}_{yf} + \hat{F}_{yr}\right)\right) + L_{12}\left(\tau_a - \hat{\tau}_a\right). \end{aligned} \tag{20}$$

$$\dot{\hat{\mu}} = L_{21}\left(\left|ma_y\right| - \left|\hat{F}_{yf} + \hat{F}_{yr}\right|\right) + L_{22}\left(\left|\tau_a\right| - \left|\hat{\tau}_a\right|\right). \tag{21}$$

In (21), we introduce absolute operators so that the gains do not change signs as the signs of lateral acceleration and aligning torque change. In (20), however, we do not need any change in the equation because α_f can have both negative and positive values, whereas μ has only positive value. The robust gains we chose are

$$L_{11} = K_1\frac{1}{mu}, \; L_{12} = K_2\frac{a}{I_z u}, \; L_{21} = K_3, \; L_{22} = K_4, \tag{22}$$

where K_1, K_2, K_3, and K_4 are all constant and $K_1<1$, $K_2>0$, $K_3>0$, $K_4>0$.

To analyze the stability of the robust observer described in (20) and (21) with the robust gains, (22), we assume the following:

$$\mathrm{sgn}(\alpha_f) = \mathrm{sgn}(\hat{\alpha}_f), \quad \mathrm{sgn}(a_y) = \mathrm{sgn}(\hat{F}_{yf} + \hat{F}_{yr}). \tag{23}$$

which are not difficult to achieve in practice by using sensor measurements judicially. The linearized equations of (20) and (21) are the same as (10) except for the observer gain matrix L. Depending on the sign of α_f and the sign of a_y, the observer has four different dynamics resulting in four sets of L matrices with one dynamic vector equation for the purpose of analysis.

$$\dot{\hat{x}} = A\hat{x} + Bu + L(y - \hat{y}) \tag{24}$$

where

$$L = \begin{cases} \begin{pmatrix} L_{11} & L_{12} \\ -L_{21} & L_{22} \end{pmatrix}, & \text{if} \quad a_y < 0, \; \alpha_f \geq 0 \\ \begin{pmatrix} L_{11} & L_{12} \\ -L_{21} & -L_{22} \end{pmatrix}, & \text{if} \quad a_y < 0, \; \alpha_f < 0 \\ \begin{pmatrix} L_{11} & L_{12} \\ L_{21} & L_{22} \end{pmatrix}, & \text{if} \quad a_y \geq 0, \; \alpha_f \geq 0 \\ \begin{pmatrix} L_{11} & L_{12} \\ L_{21} & -L_{22} \end{pmatrix}, & \text{if} \quad a_y \geq 0, \; \alpha_f < 0 \end{cases}$$

Equation (21), in fact, is not differentiable at the x where assumption (23) is not satisfied. The assumption, (23), is not true when α or a_y is very small, and is detectable using sensor measurements. Thus, (21) is piece-wisely differentiable. However, we can analyze the stability of the observer in each continuous region. The observer may or may not be stable

when the assumption is not true. However, the stability analysis is not presented here. Friction estimation when α or a_y is very small is not critical for the active safety systems and is generally challenging to dynamic based estimation methods because of small excitation. Thus, consider the case that (23) is true not the case of small excitation. We check the two stability conditions considering practical vehicle parameters and variable ranges, such as vehicle longitudinal speed, front and rear tire slip angle, and road steer angle. For example, when sign of α_f and the sign of a_y are both positive, the first and second condition are

$$\begin{aligned} D_{11}+D_{22} &= \frac{1-K_1}{mu}\frac{\partial F}{\partial \alpha_f}+\frac{a}{I_z u}\frac{\partial M}{\partial \alpha_f} \\ &\quad -K_2\frac{a}{I_z u}\frac{\partial \tau_a}{\partial \alpha_f}-K_3\frac{\partial F}{\partial \mu}-K_4\frac{\partial \tau_a}{\partial \mu}<0, \end{aligned} \tag{25}$$

$$\begin{aligned} &D_{11}D_{22}-D_{12}D_{21} \\ &=\left(\frac{(1-K_1)}{mu}K_4+K_2K_3\frac{a}{I_z u}\right)\left(\frac{\partial F}{\partial \mu}\frac{\partial \tau_a}{\partial \alpha_f}-\frac{\partial F}{\partial \alpha_f}\frac{\partial \tau_a}{\partial \mu}\right) \\ &\quad +\frac{a}{I_z u}K_4\left(\frac{\partial M}{\partial \mu}\frac{\partial \tau_a}{\partial \alpha_f}-\frac{\partial M}{\partial \alpha_f}\frac{\partial \tau_a}{\partial \mu}\right) \\ &\quad -K_3\frac{a}{I_z u}(a+b)\left(\frac{\partial F_{yf}}{\partial \alpha_f}\frac{\partial F_{yr}}{\partial \mu}-\frac{\partial F_{yf}}{\partial \mu}\frac{\partial F_{yr}}{\partial \alpha_f}\right)>0, \end{aligned} \tag{26}$$

where

$$F=F_{yf}+F_{yr},\ M=aF_{yf}-bF_{yr}.$$

Selecting K_1, K_2, K_3, and K_4, which meet (25), (26), is not always possible. Thus we focus on practical variable ranges, as follows:

$$u<300\,\text{km/h},\ \delta<30\,\text{deg},\ 0<\mu<1.2. \tag{27}$$

Also, for simplicity, we consider the limited range of slip angles as follows:

$$0<\alpha_f<\alpha_{fsl},\ 0<\alpha_r<\alpha_{rsl}. \tag{28}$$

Then we expand the range of slip angles and perform stability analysis for the whole slip angle range. Sufficient conditions to meet (25) and (26) are easily calculated by plugging (3) and (4) into (25) and (26). The sufficient conditions are

$$\begin{aligned} &\frac{1-K_1}{m}-\frac{ab}{I_z}>0,\ P_2-P_1>\frac{4P_2^2}{P_3},\ P_3-3P_2-P_1>0, \\ &0<\frac{P_6}{P_4+aP_5}<1,\ K_4\ge\frac{amK_2K_3}{abm-I_z(1-K_1)}, \end{aligned} \tag{29}$$

where

$$P_1=(1-K_1)/(mu)+a^2/(I_z u),$$

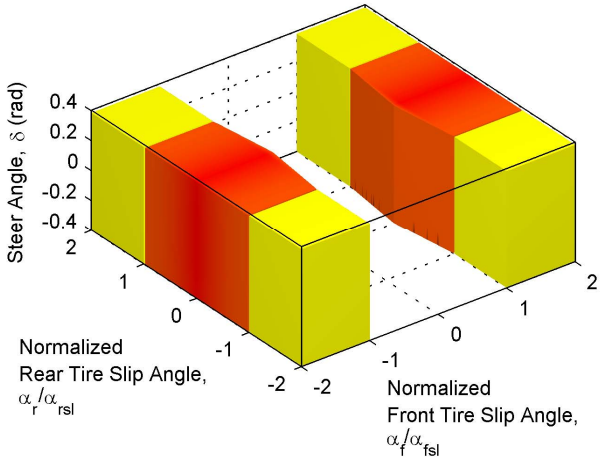

Fig. 1. Stability space of the nonlinear observer with the robust gains. The observer is unstable in the red space, neutral in the yellow space, and stable in the transparent space. α_{fsl} and α_{rsl} are the front and rear tire slip angle at which the tires begin to completely slide, respectively.

$$\begin{aligned} P_2&=K_2a^2/(3I_z u),\\ P_3&=3K_4F_z t/C_{\alpha f},\\ P_4&=(1-K_1)K_4/m+aK_2K_3/I_z,\\ P_5&=aK_4/I_z,\\ P_6&=-a(a+b)K_3/I_z. \end{aligned}$$

Using the vehicle parameters described in Table I and the sufficient conditions (28), we obtain

$$K_1=-0.678,\ K_2=47.97,\ K_3=0.001,\ K_4=0.2. \tag{30}$$

Even though these observer gains are obtained with limited variable range (28), if we expand the range into whole range, i.e., into any α_f and α_r, the first condition is always met if it is under the conditions (27). The second condition is not always satisfied, but the unstable range of variables can be calculated, as shown in Fig. 1 which shows stability in the α_f-α_r-δ coordinate. The observer is unstable in the red space, neutral in the yellow space, and stable in the transparent space.

In the red (unstable) space, the front tires completely slide ($\alpha_f/\alpha_{fsl} > 1$) whereas rear tires' friction potential still remains ($\alpha_r/\alpha_{rsl} < 1$)—a condition known as critical understering. In

TABLE I
VEHICLE AND TIRE PARAMETERS

Parameter	Value	Unit	Description
m	1412	kg	Vehicle mass
I_z	1523	kg·m^2	Moment of inertia
a	1.016	m	Distance from front axle to the center of mass
b	1.562	m	Distance from rear axle to the center of mass
t	0.178	m	The half of tire contact length
C_{af}	5000	N/rad	Cornering stiffness

other words, if the vehicle's front tires are completely sliding and rear tires are not, then we cannot estimate α_f and μ. This is a limitation of the robust observer. We can also find other unstable cases when the assumption (23) is not satisfied. These instabilities occur when α_f or a_y is very small. This instability happens more easily than critical understeering previously described. However, in this case we can disable the observer because the instance is very short or safety systems will not be activated because vehicle is driving straight. In the yellow space, i.e. if the observer is neither stable nor unstable, the observer has a negative egien value and a zero egien value. In this space, actually, α_f is unobservable, whereas μ is observable because the elements of the first column in the C matrix of (9) are all zero but the elements of the second column are not.

In summary, the robust gain design approach is practical and the criteria for robust stability are clearly understood. However, it still has limitations, especially when α_f or a_y have small magnitude.

IV. Hybrid Observer

We introduced two nonlinear observers using different gains and suggested nonlinear least square method in [1]. Nonlinear least square method has the advantage in that estimated frictional coefficient is not sensitive to current noisy measurement because the estimator utilizes past data to estimate the current frictional coefficient. Because of this, the estimation response is slow, and in addition, getting the best estimates of slip angle is not always guaranteed due to the inherent weakness of least square methods. Whereas, nonlinear observers show better slip angle estimation performance and has fast estimation response to road surface change. Nevertheless, this estimator shows unstable estimation when α_f or a_y stays around zero.

Hybrid observer combines the two algorithms to compensate for the disadvantages of each estimator. This procedure is described in Fig. 2. Nonlinear least square method uses tire slip angle estimated by nonlinear observer so that it does not need to estimate slip angles and frictional coefficient at the same time. Eliminating unknowns lowers the possibility of stalling around a local minimum and reduces computational load.

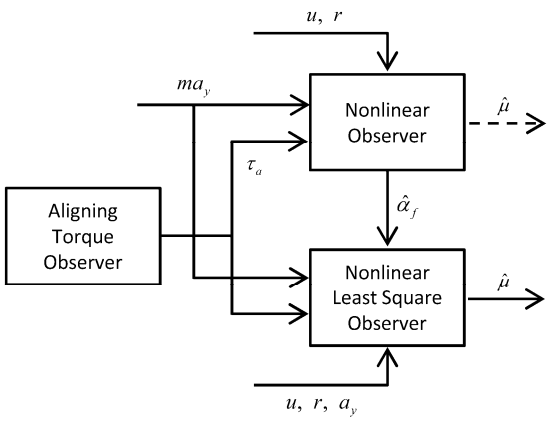

Fig. 2. Procedure of Hybrid Observer

The unknown variable in the nonlinear least square observer embedded the Hybrid observer is only a frictional coefficient because front tire slip angles are produced from the nonlinear observer and provided to nonlinear least square estimator, making it much easier to find a better frictional coefficient.

V. Simulation Results

We verified the algorithms with Carsim with three levels of frictional coefficients. The vehicle speed is 60 km/h and steer input is 0.25Hz sine wave with a magnitude of 0.04 rad. The observer using adaptive gains shows overall stable and acceptable result through all friction levels. On a low frictional road, the observer fluctuates when α_f is around zero, as show Fig. 5, because estimated values and real values of α_f and μ are different. The observer using robust gains estimates both α_f and μ well, but shows an unstable estimation performance when α_f is close to zero. This result is consistent with the stability analysis of the previous section. Even though robust gains depend on vehicle speed only and not on estimated α_f or μ, the observer using robust gains has equivalent performance and stability as the observer using adaptive gains. The hybrid estimator shows the best performance among the three algorithms. As shown in Fig. 4 and Fig. 5, the hybrid estimator has smooth and accurate estimations.

On a high friction road, all three observers estimate α_f on the high friction road very well, whereas, they overestimate μ. However, on a low friction road, such as when frictional coefficient is 0.5 or 0.2, the error variation of estimated friction is smaller than that on a high friction road, even though the slip angle estimation is worse than that of the high friction road case; vehicle motion easily becomes nonlinear with a large slip angle on a low friction road so that the slip angle estimation is not accurate. Nevertheless, the frictional coefficient on low friction roads is easily identified, because tire characteristic curves are more separated when frictional

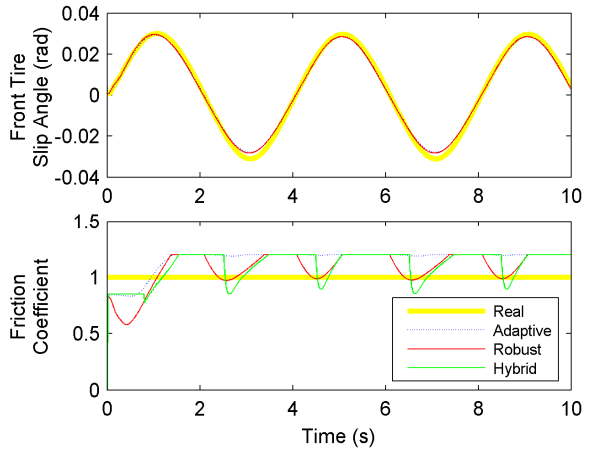

Fig. 3. Simulation result when frictional coefficient is 1.0. Adaptive means the Nonlinear Observer using adaptive gains, Robust means the Nonlinear Observer using robust gains, and Hybrid means the Hybrid Estimator.

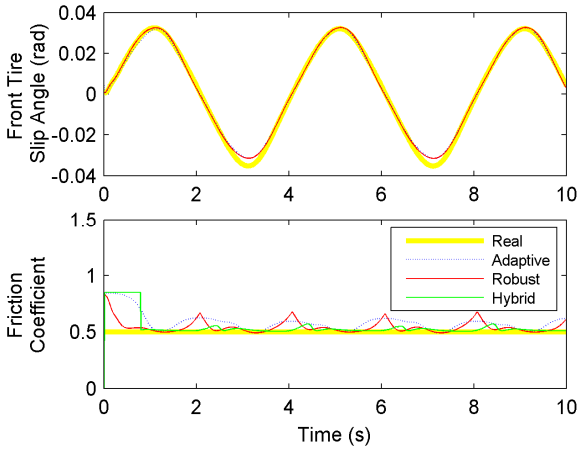

Fig. 4. Simulation result when frictional coefficient is 0.5.

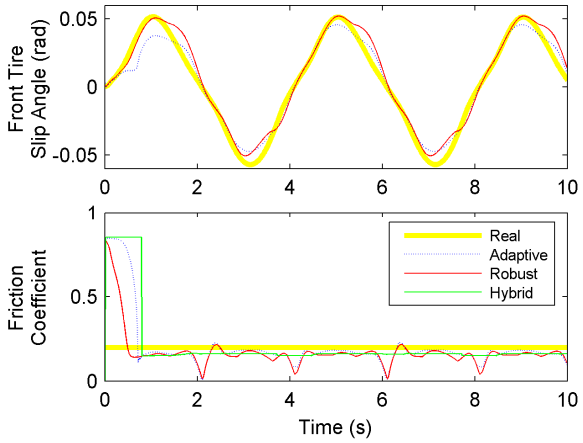

Fig. 5. Simulation result when frictional coefficient is 0.2.

coefficient is small, whereas the curves aggregate densely if the frictional coefficient is large, as shown in Fig. 6. In other words, tire characteristic curves become insensitive to slip angle change and become sensitive to frictional coefficient change as the frictional coefficient becomes smaller. As shown in Fig. 7, all the partial derivatives to frictional coefficient are zero when slip angle is zero, whereas, all the partial derivatives to slip angle have the largest values when slip angle is zero.

VI. Conclusion

This paper presents three estimators for the coefficient of friction between road and tire. Nonlinear observers based on stable observer design produced good results except that unstable estimation may occur when the slip angle or lateral acceleration is small. To utilize the advantages of nonlinear least square method described in [1] and to overcome the disadvantages of the nonlinear observers explained in this paper, we introduce a Hybrid Estimator which combines the two methods and demonstrates an overall stable and robust performance.

Robustness analysis and systematic gain selection methods were not presented in this paper. We will conduct a study on

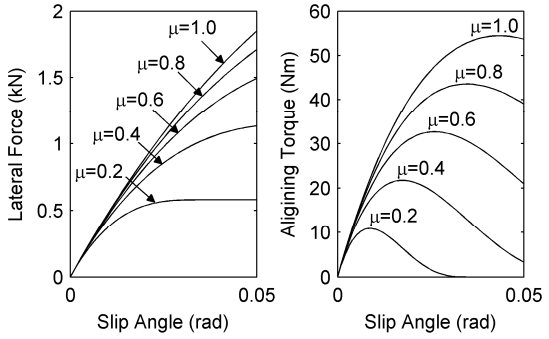

Fig. 6. Effect of friction coefficient on tire characteristics

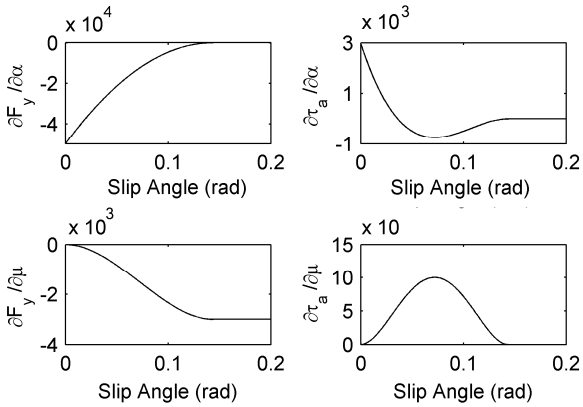

Fig. 7. Partial derivatives of tire force and torque equations

the topics and present it in the future.

References

[1] C. Ahn *et al.*, "Estimation of Road Friction for Enhanced Active System: Dynamics Based Approach,"in *Proc. 2009 American Control Conference*, St. Louis, Missouri, 2009.

[2] Y. Hsu and J. C. Gerdes, "A feel for the road: a method to estimate tire parameters using steering torque," in *Proc. Int. symp. Advanced Vehicle Control*, Taipei, Taiwan, 2006. pp. 1-6.

[3] C. Canudas-de-Wit, "A new nonlinear observer for tire/road distributed contact friction," in *Proc. 42nd IEEE Conf. Decision and Control, Maui*, Hawaii, 2003, vol. 3, pp. 2246–2251.

[4] Y. Hsu *et al.*, "A method to estimate the friction coefficient and tire slip angle using steering torque," in *Proc. 2006 ASME Int. Mech. Eng. Congr. Expo.*, Chicago, Illinois, 2006, pp. 1-10.

[5] L. Ray, "Nonlinear tire force estimation and road friction identification: simulation and experiments," *Atomatica*, vol. 33, no. 10, pp. 1819-1833, Oct. 1997.

[6] G. Baffet *et al.*, "Experimental evaluation of observers for tire-road forces, sideslip angle and wheel cornering stiffness," *Vehicle System Dynamics*, vol. 46, no. 6, pp. 501–520, Jun. 2008.

[7] J. Dakhlallah, *et al.*, "Tire-road force estimation using extended kalman filter and sideslip angle evaluation," in *Proc. 2008 American Control Conference*, Seattle, Washington, 2008, pp. 4597-4602.

[8] Y. Yasui *et al.*, "Estimation of lateral grip margin based on self-aligning torque for vehicle dynamics enhancement," in *SAE 2004 World Congress & Exhibition*, Detroit, USA, 2004, paper no. 2004-01-1070.

[9] E. Ono, "Estimation and control of vehicle dynamics for active safety," *R&D Review of Toyota CRDL*, vol. 40, no. 4, pp. 1-6, Sep. 2005.

[10] E. Ono *et al.*, "Estimation of tire friction circle and vehicle dynamics integrated control for four-wheel distributed steering and four-wheel distributed traction/braking systems," *R&D Review of Toyota CRDL*, vol. 40, no.4, pp.7-13, Sep. 2005.

[11] T. Umeno, "Detection of tire lateral force based on a resolver mechanism," *R&D Review of Toyota CRDL*, vol. 40, no.4, pp.14-19, Sep. 2005.